

Cite this: *J. Mater. Chem.*, 2011, **21**, 15660

www.rsc.org/materials

PAPER

# Phosphoric acid-doped cross-linked porous polybenzimidazole membranes for proton exchange membrane fuel cells

Cheng-Hsun Shen, Li-cheng Jheng, Steve Lien-chung Hsu\* and Jacob Tse-Wei Wang

Received 21st June 2011, Accepted 9th August 2011

DOI: 10.1039/c1jm12857d

Cross-linked porous polybenzimidazole (PBI) membranes were prepared by mixing a low-molecular-weight compound (porogen) and a cross-linker with the polymer to form cross-linked polymer membranes in order to increase the mechanical strength and proton conductivity. SEM images of the cross-section of the porous polymer membranes show the pore size and morphology. The cross-linking by *p*-xylylene dichloride can effectively improve the mechanical properties of the porous PBI membranes after phosphoric acid doping. The CpPBI-60 membrane, which is doped with 9 moles of phosphoric acid, has a tensile modulus of 0.45 GPa. The good mechanical strength of the cross-linked porous PBI membranes makes them able to hold more phosphoric acid and, consequently, have higher proton conductivity. Fenton's test indicated that the covalently cross-linked structure played an important role in the radical oxidative stability of the porous membranes. The doping level of phosphoric acid in the cross-linked porous PBI membranes showed that the enhanced conductivity was due to the increase of porosity, which results in the increase of acid uptake. Impedance analysis showed that the conductivity of the cross-linked porous PBI membranes could reach  $2.1 \times 10^{-2} \text{ S cm}^{-1}$  at 160 °C under anhydrous conditions.

## 1. Introduction

The proton exchange membrane (PEM) is one of the key components for polymer exchange membrane fuel cells (PEMFCs). In PEMFCs, the proton conducting polymer is used in the form of a thin film and acts as a solid electrolyte. PEMs require chemical stability, thermal stability, ability to be electrically insulating, ability to restrict fuel crossover, and outstanding mechanical properties, as well as low cost fabrication for useful applications. Polybenzimidazole (PBI) membranes exhibit good characteristics at temperatures up to 200 °C.<sup>1–7</sup> In particular, PBI doped with phosphoric acid (PA) has stable proton conductivity at temperatures higher than 100 °C, which gives it the potential for use as a high-temperature proton exchange membrane.<sup>8–15</sup> The proton conductivity of PA-doped PBI membranes was dependent on the doping level. The conventional PA-doped PBI membranes were prepared by immersing the PBI membranes in a PA solution. Several different processes for preparation of PA-doped PBI membranes have been explored to improve the proton conductivity in recent years. Recently, Mecerreyes *et al.* proposed a method to increase the PA-doping level in PBI membranes by incorporating porosity with different porogens.<sup>16</sup> Using this method, the acid uptake increased from the value of

132% for pure PBI up to 439% for a porous PBI membrane containing 70% dibutyl phthalate. The conductivity of the porous PBI reached a maximum value of  $5 \times 10^{-2} \text{ S cm}^{-1}$  at high temperatures. Also, several research groups have developed new methods to generate PBI membranes to exhibit high conductivity, such as by direct casting methods. For example, PBI membranes were prepared by direct-casting from a PBI/methanesulfonic acid solution to obtain high acid-doping levels, which could reach as high as 30–40 PA/PBI repeat unit.<sup>17</sup> However, one of the drawbacks of PBI membranes doped with high amounts of PA is the extremely poor mechanical properties to fabricate membrane electrode assemblies. To solve this issue, covalent cross-linked PBI had been demonstrated to be a useful approach.<sup>18–21</sup> Cross-linked PBI membranes with both outstanding mechanical stability and high proton conductivity have been successfully prepared.<sup>22–24</sup>

In this work, we report the preparation of cross-linked and porous PBI membranes for PEM. By combining the porosity and cross-linking approaches, we were able to prepare new PBI membranes with high proton conductivity at high temperatures and useful mechanical properties after PA doping.

## 2. Experimental

### Materials

2,2-Bis(4-carboxyphenyl)hexafluoropropane was purchased from TCI. 3,3-Diaminobenzidine, dimethylacetamide, 1,4-bis

Department of Materials Science & Engineering, Research Center for Energy Technology and Strategy, National Cheng-Kung University, Tainan, 701-01 Taiwan, R.O.C. E-mail: lchsu@mail.ncku.edu.tw; Fax: +886 6 2346290; Tel: +886 6 2757575 ex 62904

(chloromethyl)benzene, ferrous sulfate, and dibutyl phthalate (DBP) were obtained from Aldrich. 3,3-Diaminobenzidine was used as received and dimethylacetamide was purified by distillation over calcium hydride. Reagent-grade poly(phosphoric acid) (PPA) and phosphoric acid (PA) were obtained from Fluka and used as supplied. Other chemicals and solvents were used as received.

### Synthesis of polybenzimidazole

In a three-necked flask equipped with a mechanical stirrer and a condenser, 5.356 g (25 mmol) of 3,3-diaminobenzidine was dissolved in 288 g of PPA. The solution was stirred until it became homogeneous. To the solution, 9.806 g (25 mmol) of 2,2-bis(4-carboxyphenyl) hexafluoropropane was added and the mixture was reacted at 200 °C for 24 h. The detailed synthetic procedure was reported in our previous paper.<sup>25</sup>

### Preparation of porous polybenzimidazole membranes

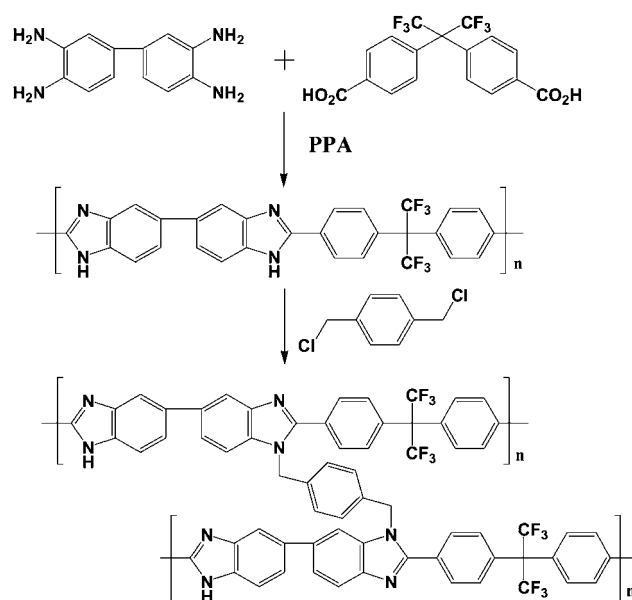
A typical preparation of pPBI-33 (pPBI-33 denotes a porous PBI with a porogen content of 33 wt%) proceeds as follows: 1.0 g of PBI was dissolved into DMAc to make a 3 wt% homogeneous solution. To the solution, 0.5 g of DBP (porogen) was added. Membranes were obtained by casting the solution onto glass plates with a doctor's knife and then dried at 80 °C for 12 h. After that, the DBP was extracted by immersing the membranes in methanol for 4 h. The porous PBI membranes were obtained by drying in vacuum at 60 °C overnight. The synthesis of pPBI-50 (DBP content of 50 wt%) and pPBI-67 (DBP content of 67 wt%) followed the same procedure with different DBP contents. The thickness of all porous PBI membranes was approximately 40 µm.

### Preparation of cross-linked porous polybenzimidazole membranes

A 3 wt% PBI solution in DMAc with a DBP (porogen) content of 33 wt% was mixed with a certain amount of cross-linker (*p*-xylylene dichloride) in a three-neck round-bottom flask. The molar ratio of the cross-linker to the amino group in the imidazole ring of PBI was controlled in the range of 0.3–0.6. (CpPBI-30, CpPBI-45, and CpPBI-60 denote cross-linked porous PBIs with a molar ratio of 0.3, 0.45, and 0.6, respectively.) The cross-linked porous PBI membranes were obtained by casting the solution onto glass plates with a doctor's knife and then dried at 120 °C for 2 h. The process of removing the DBP was the same as the process mentioned above. The thickness of all cross-linked porous PBI membranes was approximately 40 µm. The synthetic and cross-linking procedures of PBI are shown in Scheme 1.

### Acid doping of polybenzimidazole membranes

All membranes were doped by immersing them in aqueous PA (14 M) for 4 days and the absorbed water was removed in an oven at 100 °C for 12 h. The amount of PA in each membrane was calculated by weight analysis. The acid-doping level ( $x$ ) of the membrane was calculated as the molar number of PA per repeat unit of PBI, which was calculated by using the following equation:



**Scheme 1** Synthesis of PBI in PPA and cross-linking of PBI by *p*-xylylene dichloride.

$$X = \frac{(W_{\text{doped}} - W_{\text{undoped}}) / M_{\text{PA}}}{(W_{\text{undoped}} / M_{\text{p}})}$$

where  $W_{\text{doped}}$  and  $W_{\text{undoped}}$  are the weights of the doped and undoped membranes, while  $M_{\text{PA}}$  is the molecular weight of PA and  $M_{\text{p}}$  is the molecular weight of the polymer repeat unit, respectively.

### Characterization

The IR spectra were recorded on a Jasco 460 FTIR spectrometer. The mechanical properties of the membranes were determined from stress–strain curves obtained with a Shimadzu AG-SI universal testing machine at a strain rate of 5 mm min<sup>−1</sup> at room temperature. The size of film specimens was 30 mm in length, 4.5 mm in width, and 40 µm in thickness. The proton conductivities were achieved with an Autolab PGSTST 30 impedance analyzer in the frequency range from 100 to 10<sup>5</sup> Hz with an amplitude of 10 mV. The measured data were collected at various temperatures from 80 to 160 °C. The proton conductivity ( $\sigma$ ) was calculated by the following equation:

$$\sigma = \frac{L}{RA}$$

where  $L$  is the distance between the two electrodes,  $R$  is the resistance of the membrane, and  $A$  is the cross-sectional area of the membrane. The cross-section of PBI films was inspected by the Phillips XL-40FEG high-resolution field emission scanning electron microscopy (FESEM).

The AccuPyc 1330 was used to measure the density of the solid polymer. The AccuPyc 1330 uses helium (99.995%) to size up the volume of the sample by measuring the pressure change of helium in the cell volume. The density  $\rho_{\text{m}}$  of polymer films was calculated by using the following equation<sup>26</sup>:

$$\rho_m = \frac{m_s}{V_c - (V_{\text{exp}} / ((p_{1G} / p_{2G}) - 1))} \left( \frac{\text{g}}{\text{cm}^3} \right)$$

where  $m_s$  is the sample mass,  $V_c$  is the cell volume,  $V_{\text{exp}}$  is the expanded volume,  $p_{1G}$  is the cell elevated pressure, and  $p_{2G}$  is the cell intermediate pressure.

The porosity of the porous membranes was measured by dipping the membranes into *n*-butanol for 1 h. The weight differences of the membranes before and after *n*-butanol absorption were measured. Then, the porosity can be calculated from the following equation:<sup>27</sup>

$$P\% = \frac{M_n / \rho_n}{M_p / \rho_p + M_n / \rho_n} \times 100\%$$

where  $P\%$  is the porosity of the membrane,  $M_n$  is the mass of *n*-butanol,  $M_p$  is the mass of membrane,  $\rho_p$  is the density of the membrane, and  $\rho_n$  is the density of *n*-butanol.

The oxidative stability was investigated by Fenton's test. The membranes were immersed into 3% hydrogen peroxide containing 4 ppm ferrous sulfate at 80 °C. We can estimate the degradation of PBI membranes by the weight loss and visual observation.

### 3. Results and discussion

#### Preparation of porous PBI and cross-linked porous membranes

Porous PBI membranes were prepared by blending DBP (porogen) into a PBI solution and the DBP was removed from the films by soaking the membranes in methanol to generate the porous membranes. The cross-linked porous PBI membranes were prepared from the reaction of *p*-xylylene dichloride, used as a cross-linking agent, with the N–H functional groups in the imidazole ring of PBI. Table 1 summarizes the properties of the porous PBI membranes prepared from DBP with 33, 50, and 67 wt% content and the cross-linked porous PBI membranes prepared with 33 wt% DBP in different amounts of cross-linker. We have also prepared cross-linked porous PBI membranes with higher DBP content, but these membranes did not have good mechanical properties and were not transparent due to phase separation. Therefore, for the cross-linked porous PBI membranes, we only focused on porous membranes with 33 wt%

**Table 1** Properties of porous PBI and cross-linked porous PBI membranes

Sample	Initial DBP content (wt%) <sup>a</sup>	Weight loss (%) <sup>b</sup>	Molar ratio of cross-linker <sup>c</sup>	Density <sup>d</sup> /g cm <sup>-3</sup>	Porosity (%)
pPBI-33	33.0	31.3	—	1.195	28.7
pPBI-50	50.0	46.6	—	1.002	47.7
pPBI-67	67.0	66.5	—	0.876	68.5
CpPBI-30	33.0	28.8	0.30	1.127	36.4
CpPBI-45	33.0	32.9	0.45	1.114	37.7
CpPBI-60	33.0	31.4	0.60	1.128	37.8

<sup>a</sup> According to  $W_{\text{DBP}} / (W_{\text{PBI}} + W_{\text{DBP}})$ , where  $W_{\text{DBP}}$  is the mass of DBP and  $W_{\text{PBI}}$  is the mass of PBI. <sup>b</sup> % Weight loss after removing the DBP by immersing the membranes in methanol for 4 h. <sup>c</sup> The molar ratio between the cross-linker *p*-xylylene dichloride and the amino group in the imidazole ring of PBI was controlled in the range of 0.3–0.6. <sup>d</sup> The density of the entire porous membrane.

DBP. After removing the DBP, the weight loss of PBI membranes was close to the initially added amounts of DBP, which indicated that the DBP was removed successfully. Apparently, the porous membranes generated from higher DBP content lead to higher porosity and lower density. AccuPyc 1330 was used to measure the density of the solid PBI. When the porosity was measured, the density of entire porous membranes could be calculated by apparent volume and weight.

#### Morphology of porous PBI membranes

Scanning electron microscopy (SEM) was used to study the surface morphology of porous PBI membranes obtained from various DBP contents. Fig. 1a–d show the cross-section of porous PBI membranes produced from DBP in zero, 33, 50, and 67 wt% content, respectively. Compared to the pristine PBI membrane with porous PBI membranes, the cross-section of pristine PBI is flat, with no defects and pores. However, at a porogen level of 33 wt%, the cross-section shows isolated spherical pores with a rough shape smaller than 5 μm. At a porogen level of 50 wt%, the surface of the membrane has irregular pores. A few of them have a cross-section diameter of more than 5 μm. At the highest porogen level of 67 wt%, larger, more irregular and interconnected pores, with a diameter between 5 and 10 μm, are more easily found. The pore size has a wide distribution from a few nanometres to a few micrometres in diameter. The shapeless and unoriented pores in these membranes may be attributed to the random dispersion of the aggregative DBP.

#### Characterization of cross-linked PBI membranes

Fig. 2 shows the FT-IR spectra of the pPBI and the cross-linked pPBI membranes. The strong absorption band from 2700 to 3500 cm<sup>-1</sup> in the pPBI is assigned to N–H groups of the imidazole

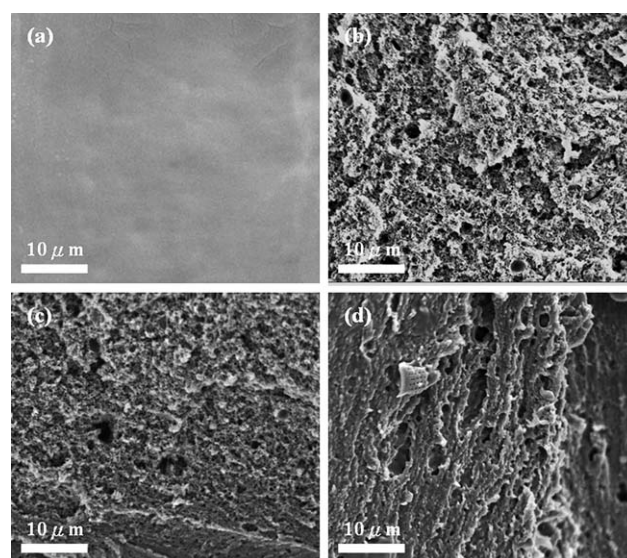


**Fig. 1** SEM micrographs of porous PBI membranes prepared from various DBP contents: (a) pristine PBI, (b) pPBI-33, (c) pPBI-50, and (d) pPBI-67.

ring. It corresponds to the stretching vibration of the N–H groups with the highest absorption intensity around  $3100\text{ cm}^{-1}$ . For the cross-linked pPBI, the absorption band at around  $2850\text{--}2750\text{ cm}^{-1}$  is assigned to the stretching vibration of the  $-\text{CH}_2-$  groups in the cross-linker units. After reacting with *p*-xylylene dichloride, many N–H groups disappeared. Therefore, the  $3100\text{ cm}^{-1}$  absorption peak of the cross-linked pPBI became weaker.<sup>19,20</sup> The characteristic absorption band at  $1630\text{ cm}^{-1}$  primarily corresponds to the C=N group stretching vibrations in the five-member heterocyclic ring of pristine PBI.<sup>25</sup>

### Mechanical properties of porous and cross-linked porous PBI membranes

The modulus, tensile strength, and elongation at break of the porous PBI and cross-linked porous PBI membranes were measured to study their mechanical properties. Fig. 3 shows that the modulus decreases with the increasing amount of DBP. It is attributed to the increasing amounts of porosity in the membranes. The pristine PBI membrane has a tensile modulus of 1.27 GPa and a tensile strength of 73.18 MPa. However, the tensile moduli of porous PBI membranes with various DBP contents of pPBI-33, pPBI-50, and pPBI-67 decreased to 0.63, 0.54, and 0.40 GPa, respectively. Their tensile stresses also have the same trend. On the other hand, the porous cross-linked PBI can overcome the drawbacks of porosity materials in mechanical properties. As shown in Fig. 4, the CpPBI-60 has a tensile modulus and a stress of 0.9 GPa and 82.9 MPa, respectively. This shows that cross-linking of PBI can improve its mechanical properties.<sup>28</sup>

The tensile properties of the cross-linked porous PBI membranes doped with 9 moles of PA are shown in Fig. 5. Compared with the cross-linked porous PBI membranes without PA, the tensile modulus and strength of the membranes decreased when they were doped with PA. This could be due to the plasticizing effect of the PA. The tensile modulus of CpPBI-30, CpPBI-45, and CpPBI-60 membranes doped with PA decreased by 57%, 56%, and 50%, respectively, with respect to the cross-linked porous PBI membranes without PA doping.

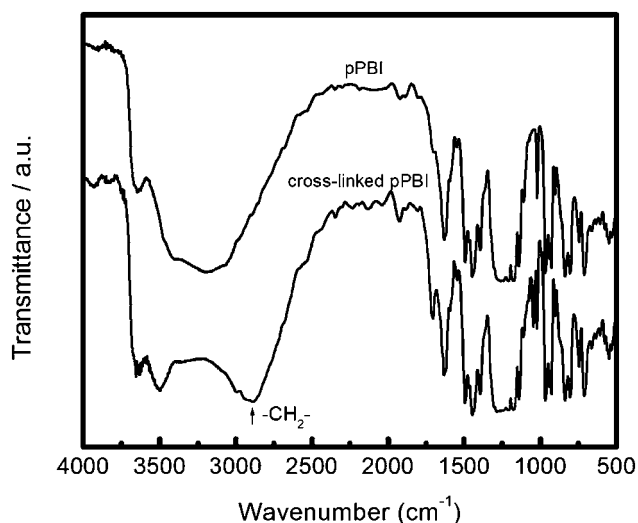


Fig. 2 FT-IR spectra of pPBI and cross-linked pPBI membranes.

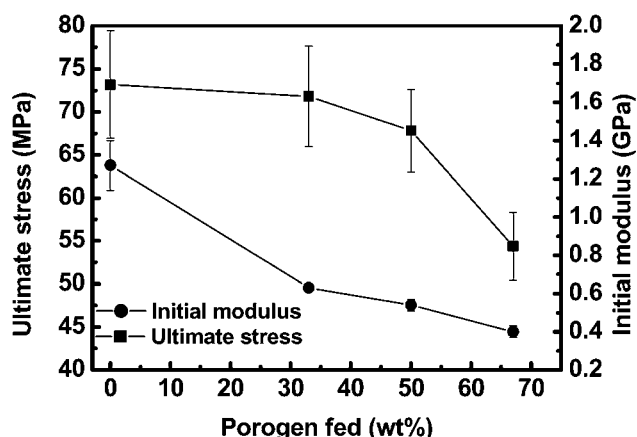


Fig. 3 The stress and modulus of PBI, pPBI-33, pPBI-50, and pPBI-67 membranes.

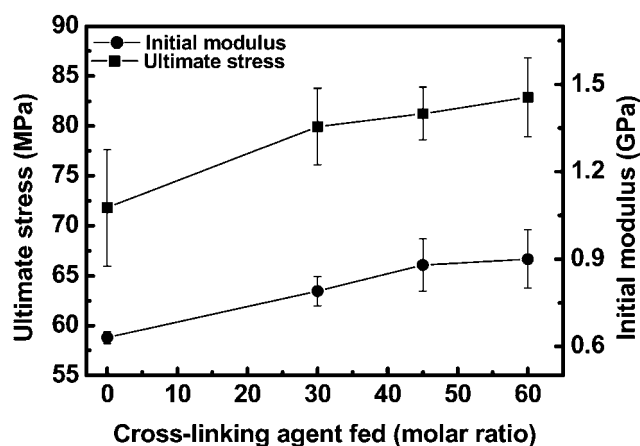


Fig. 4 The stress and modulus of pPBI-33, CpPBI-30, CpPBI-45, and CpPBI-60 membranes.

However, the acid-doped membranes still had suitable mechanical properties for use in PEMFC. It implied that the cross-linked PBI membranes could effectively restrict the plasticizing effect of

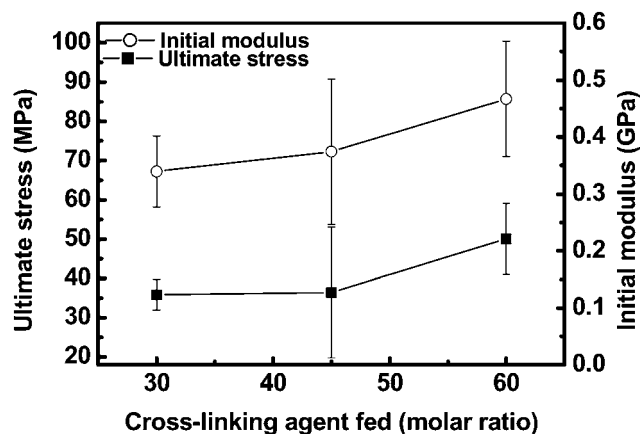


Fig. 5 The stress and modulus of CpPBI-30, CpPBI-45, and CpPBI-60 membranes doped with 9 moles of phosphoric acid.



the PA to maintain the mechanical properties of the acid-doped cross-linked porous PBI membranes.

### Chemical stability

Fenton's test is a common method for evaluating the radical oxidative stability of PEMFC. During the utilization of fuel cells, radicals such as HO $\cdot$  and HOO $\cdot$  form and attack the proton exchange membranes, which causes degradation. Therefore, polymers with hydrogen-containing bonds can be attacked by the radicals. In Fenton's test, these radicals can be produced by Fe $^{2+}$  catalyzed H $_2$ O $_2$  decomposition.<sup>29,30</sup> The results of Fenton's test are shown in Fig. 6. As can be seen from Fig. 6, the CpPBI-60 membrane showed excellent stability, with a weight loss of less than 3% after 96 h. It could also be observed that there was no weight loss in the first 24 h. For the CpPBI-45 and CpPBI-30 membranes, the samples remained intact and showed a weight loss of less than 4% after 96 h. This indicated that the cross-linked porous PBI membranes had good radical oxidative stability as expected. Non-cross-linked porous PBI membranes, pPBI-33, pPBI-50, and pPBI-67, showed a weight loss of up to 3.7%, 4.1%, and 7.2% after 96 h, respectively. Non-cross-linked porous PBI membranes with high porosity and large surface area lead to more opportunity for the free radical oxidative process. For the covalently cross-linked PBI membranes, the cross-

linking structure indeed enhanced the free radical oxidative stability.<sup>17</sup> After a longer testing period, the influence of cross-linking was more significant.

### Proton conductivity

The PA-doping level of porous PBI membranes generated by this process was much higher than other PA doped PBI membranes without porosity. The porous PBI membranes were doped with PA in a 14 M PA solution for 4 days. Obviously, the doping level (PA/PBI repeat unit) increased from the value of 4.7 for pure PBI up to 7.2, 12.5, and 13.8 for porous membranes that contain 33%, 50%, and 67% DBP, respectively, as illustrated in Fig. 7. Proton conductivity of these porous PBI membranes was measured using an ac impedance system in the temperature range of 80–160 °C. The proton conductivity of the PA-doped porous PBI membranes with different degrees of porosity is shown in Fig. 8. For the highest degree of porosity, the proton conductivity was approximately  $1.5 \times 10^{-2}$  S cm $^{-1}$  at 80 °C and reached  $3.0 \times 10^{-2}$  S cm $^{-1}$  at 160 °C without humidification. Compared with the pristine PBI membrane, the proton conductivity of the porous PBI membranes increased 20 times when the acid uptake increased 2.9 times.

The cross-linked porous PBI membranes were doped with about 9 moles of PA per PBI repeat unit. Compared with the pPBI-33 membrane which has a PA-doping level of 7.2, the CpPBI-30, CpPBI-45, and CpPBI-60 have PA-doping levels of 9.1–9.5. The PA-doping levels for cross-linked porous PBI membranes are higher than the porous PBI membranes with the same porosity, as shown in Fig. 9. The acid doped in porous PBI membranes might leak in fuel cell utilization. The cross-linking procedure could turn the PBI into a denser structure; therefore the PA molecule could be loaded firmly in the membranes.<sup>18</sup> The cross-linked porous PBI membranes have a capability to hold more PA molecules to increase the proton conductivity. Fig. 9 also shows the proton conductivity of the cross-linked porous PBI membranes doped with a similar acid-doping level. The proton conductivity of the cross-linked porous PBI membranes increases with increasing temperatures. The conductivity of cross-linked porous PBI membranes could reach  $2.1 \times 10^{-2}$  S cm $^{-1}$  at 160 °C under anhydrous conditions. For

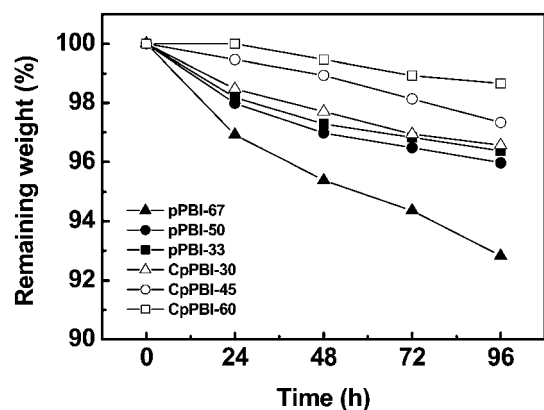


Fig. 6 Oxidative stability of PBI films with time. Membrane degradation in 3% H $_2$ O $_2$  containing 4 ppm Fe $^{2+}$  at 80 °C.

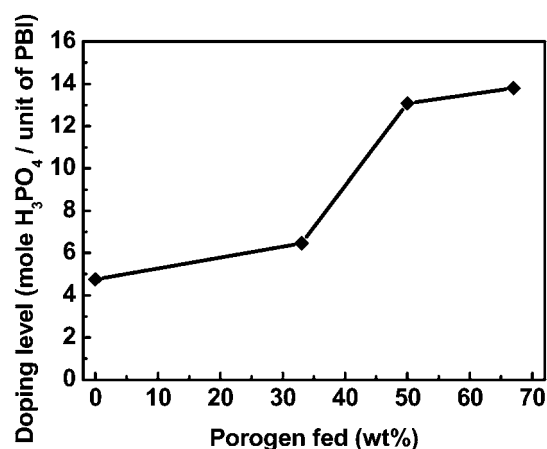


Fig. 7 Phosphoric acid-doping levels of PBI and pPBI membranes.

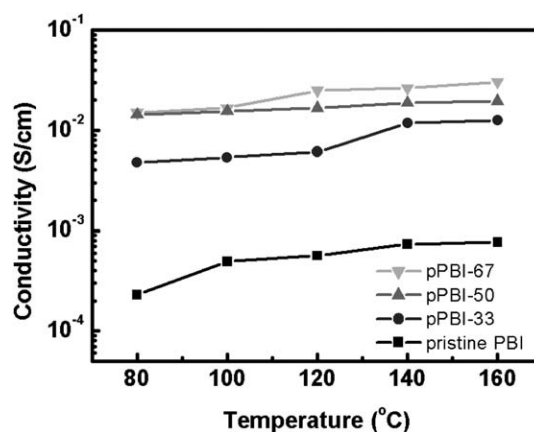


Fig. 8 Proton conductivity of PBI and pPBI membranes doped with different amounts of phosphoric acid at different temperatures.

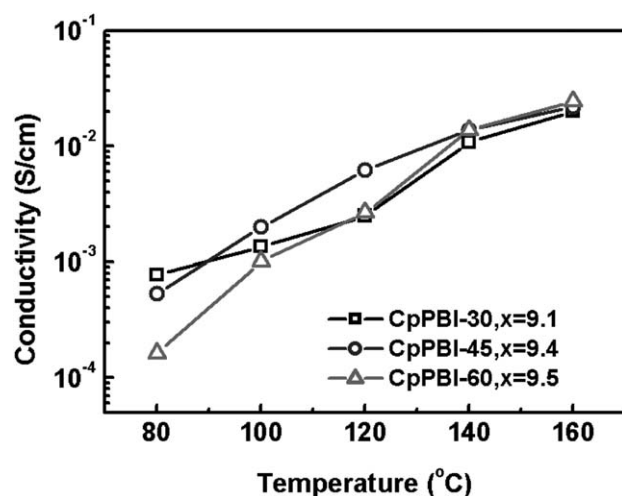


Fig. 9 Proton conductivity of cross-linked porous PBI membranes doped with different amounts of phosphoric acid at different temperatures.

membranes of CpPBI-60 with porosity 33% at an acid-doping level of 9.5 and pPBI-67 with porosity 67% at an acid-doping level of 13.8, their conductivities are very close. The cross-linked porous PBI membranes have a sufficient mechanical strength due to the cross-linker *p*-xylene dichloride. Furthermore, the cross-linked porous PBI membranes show much improved conductivity with lower porosity and acid-doping level.

#### 4. Conclusions

Cross-linked porous PBI membranes have been prepared by mixing PBI with a DBP and a cross-linker. The introduction of porosity in the membranes significantly increased the PA-doping level, which resulted in higher proton conductivity. Using *p*-xylylene dichloride to cross-link the porous PBI membranes effectively increased the mechanical properties of the membranes after PA doping and enhanced the free radical oxidative stability of the porous membranes. After doping with PA, the cross-linked porous PBI membranes showed high proton conductivity at high temperatures. The cross-linked porous PBI membranes have the potential for use as proton exchange membranes in high temperature PEMFC.

#### Acknowledgements

The financial support provided by the National Science Council through project NSC99-2923-E-006-005-MY3 is greatly appreciated.

#### Notes and references

- 1 M. Litt, R. Ameri, Y. Wang, R. Savinell and J. Wainwright, *MRS Online Proc. Libr.*, 1999, **548**, 313–323.
- 2 S. R. Samms, S. Wasmus and R. F. Savinell, *J. Electrochem. Soc.*, 1996, **143**, 1225–1232.
- 3 S. W. Chuang, L. C. Hsu and C. L. Hsu, *J. Power Sources*, 2007, **168**, 172–177.
- 4 S. W. Chuang, L. C. Hsu and M. L. Yang, *Eur. Polym. J.*, 2008, **44**, 2202–2206.
- 5 G. Qian and B. C. Benicewicz, *J. Polym. Sci., Part A: Polym. Chem.*, 2009, **47**, 4064–4073.
- 6 N. N. Krishnan, H. J. Lee, H. J. Kim, J. Y. Kim, I. C. Hwang, J. H. Jang, E. A. Cho, S. K. Kim, D. Henkensmeier, S. A. Hong and T. H. Lim, *Eur. Polym. J.*, 2010, **46**, 1633–1641.
- 7 S. G. Feng, Y. M. Shang, S. B. Wang, X. F. Xie, Y. G. Wang, Y. W. Wang and J. M. Xu, *J. Membr. Sci.*, 2010, **346**, 105–112.
- 8 M. Kawahara, J. Morita, M. Rikukawa, K. Sanui and N. Ogata, *Electrochim. Acta*, 2000, **45**, 1395–1398.
- 9 L. Xiao, H. Zhang, T. Jana, E. Scanlon, R. Chen, E. W. Choe, L. S. Ramanathan, S. Yu and B. C. Benicewicz, *Fuel Cells*, 2005, **5**, 287–295.
- 10 Suryani and Y. L. Liu, *J. Membr. Sci.*, 2009, **332**, 121–128.
- 11 A. D. Modestov, M. R. Tarasevich, V. Y. Filimonov and N. M. Zagudaeva, *Electrochim. Acta*, 2009, **54**, 7121–7127.
- 12 S. Yu, L. Xiao and B. C. Benicewicz, *Fuel Cells*, 2008, **3–4**, 165–174.
- 13 L. Xiao, H. Zhang, E. Scanlon, L. S. Ramanathan, E. W. Choe, D. Rogers, T. Apple and B. C. Benicewicz, *Chem. Mater.*, 2005, **17**, 5328–5333.
- 14 K. D. Kreuer, A. Fuchs, M. Ise and M. Spaeth, *Electrochim. Acta*, 1998, **43**, 1281–1288.
- 15 D. J. Jones and J. Rozière, *J. Membr. Sci.*, 2001, **185**, 41–58.
- 16 D. Mecerreyes, H. Grande, O. Miguel, E. Ochoteco, R. Marcilla and I. Cantero, *Chem. Mater.*, 2004, **16**, 604–607.
- 17 G. Qian, D. W. Smith and B. C. Benicewicz, *Polymer*, 2009, **50**, 3911–3916.
- 18 Q. Li, C. Pan, J. O. Jensen, P. Noyé and N. J. Bjerrum, *Chem. Mater.*, 2007, **19**, 350–352.
- 19 K. Y. Wang, Y. C. Xiao and T. S. Chung, *Chem. Eng. Sci.*, 2006, **61**, 5807–5817.
- 20 K. Y. Wang, Q. Yang, T. S. Chung and R. Rajagopalan, *Chem. Eng. Sci.*, 2009, **64**, 1577–1584.
- 21 J. Kerres, *Fuel Cells*, 2005, **5**, 230–247.
- 22 J. Kerres, W. Cui and M. Junginger, *J. Membr. Sci.*, 1998, **139**, 227–241.
- 23 J. Kerres, *Fuel Cells*, 2006, **3–4**, 251–260.
- 24 C. Zhao, H. Lin, M. Han and H. Na, *J. Membr. Sci.*, 2010, **353**, 10–16.
- 25 S. W. Chuang and L. C. Hsu, *J. Polym. Sci., Part A: Polym. Chem.*, 2006, **44**, 4508–4513.
- 26 A. Menner, K. Haibach, R. Powell and A. Bismarck, *Polymer*, 2006, **47**, 7628–7635.
- 27 C. G. Wu, M. I. Lua and H. J. Chuang, *Polymer*, 2005, **46**, 5929–5938.
- 28 T. V. Graberg, A. Thomas, A. Greiner, M. Antonietti and J. Weber, *Macromol. Mater. Eng.*, 2008, **293**, 815–819.
- 29 H. T. Pu, L. Wang, H. Y. Pan and D. C. Wan, *J. Polym. Sci., Part A: Polym. Chem.*, 2010, **48**, 2115–2122.
- 30 G. M. Zhang, X. X. Guo, J. H. Fang, K. C. Chen and K. I. Okamoto, *J. Membr. Sci.*, 2009, **326**, 708–713.